

# 1,1,2-Tri-*tert*-butyldisilane, $\text{Bu}^t_2\text{HSiSiH}_2\text{Bu}^t$ : vibrational spectra and molecular structure in the gas phase by electron diffraction and *ab initio* calculations †

Sarah L. Hinchley,<sup>a</sup> Bruce A. Smart,<sup>a</sup> Carole A. Morrison,<sup>a</sup> Heather E. Robertson,<sup>a</sup> David W. H. Rankin,<sup>\*a</sup> Robert Zink<sup>b</sup> and Karl Hassler<sup>\*b</sup>

<sup>a</sup> Department of Chemistry, University of Edinburgh, West Mains Rd., Edinburgh, UK EH9 3JJ

<sup>b</sup> Institut für Anorganische Chemie, Technische Universität Graz, Stremayrgasse 16, A-8010 Graz, Austria

Received 24th March 1999, Accepted 3rd June 1999

The molecular structure of 1,1,2-tri-*tert*-butyldisilane,  $\text{Bu}^t_2\text{HSiSiH}_2\text{Bu}^t$ , has been determined in the gas phase by electron diffraction (GED) and *ab initio* molecular-orbital calculations. Vibrational spectra are consistent with a vapour consisting of one conformer, identified by the structural study as a *syn* arrangement in which each of the butyl groups eclipses an Si–H bond. Important structural parameters ( $r_a$ ) for the conformer are: Si–Si 236.3(8), Si–C (mean) 191.1(3), C–C 154.5(1), C–H 112.4(1) pm, Si(1)–Si(2)–C(21) 116.0(8), Si(2)–Si(1)–C(11) 111.2(10), Si(2)–Si(1)–C(12) 108.7(9), C(11)–Si(1)–C(12) 121.1(11) and C(21)–Si(2)–Si(1)–H(13)  $-6.2(11)^\circ$ , where C(11), C(12) and C(21) are the central carbon atoms of the three *tert*-butyl groups. These experimental observations are supported by theoretical predictions obtained at the D95\*/MP2 level, which also identify two higher-energy conformers.

## Introduction

The electronic spectra of peralkylated silicon backbone polymers in the near-UV region have been found to be surprisingly sensitive to conformational properties of the compound under investigation.<sup>1</sup> Considerable variations of the absorption bands are observed as a function of conformation about the Si–Si backbone for both polysilanes and short-chain silanes.<sup>2</sup> The structures of some simple disilanes including  $\text{Si}_2\text{H}_6$  and  $\text{Si}_2\text{Cl}_6$  have been determined previously,<sup>3</sup> as have the structures of some partially halogenated disilanes such as 1,1,2,2-tetrabromodisilane,<sup>4</sup> 1,2-diiododisilane<sup>5</sup> and 1,1,2,2-tetraiododisilane.<sup>5</sup> Recently, more sterically crowded systems containing *tert*-butyl groups were studied including 1,2-di-*tert*-butyldisilane,<sup>6</sup> 1,2-di-*tert*-butyltetrafluorodisilane<sup>7</sup> and 1,2-di-*tert*-butyltetrachlorodisilane.<sup>8</sup>

*Ab initio* computations have been performed on all of these compounds and, as might be expected on steric grounds, the *anti* conformation is favoured in all cases. The 1,2-di-*tert*-butyltetrachlorodisilane is predicted to exhibit three local minima on the potential energy surface at the 6-31G\*/MP2 level, with C–Si–Si–C dihedral angles of 56, 94 and  $169^\circ$ , the *anti* conformer being slightly distorted from the idealised structure. In contrast, for 1,2-di-*tert*-butyldisilane only two conformers were located at the 6-31G\*/SCF level, *anti* and *gauche* (C–Si–Si–C dihedral angles of 176.8 and  $69.0^\circ$  respectively). The energy minimum for the *gauche* structure of 1,2-di-*tert*-butyldisilane was estimated to lie  $5.4 \text{ kJ mol}^{-1}$  above that for the *anti* structure on the potential energy surface and therefore the *gauche* structure should not be observable by electron diffraction in the gas phase. It was not possible to determine from the GED data how much of the *gauche* conformer was present,

although it was certainly less than 20%. For 1,2-di-*tert*-butyltetrafluorodisilane two conformers, *gauche* and *anti*, were predicted from calculations at the 6-31G\*/SCF level, with vibrational frequency calculations indicating that both forms represent local minima. However, the barrier to interconversion between *gauche* and *anti* was predicted to lie just  $0.25 \text{ kJ mol}^{-1}$  above the *gauche* isomer, which may therefore represent a quasi-minimum on the potential energy surface rather than a distinct conformer. The experimental structure was modelled with two conformers, but as the C–Si–Si–C dihedral angles refined to  $184(7)$  and  $152(3)^\circ$ , the data are consistent with a single conformer with a large-amplitude motion over a torsional range of around  $140\text{--}220^\circ$  rather than with a mixture of two distinct conformers.

In view of the interesting conformational behaviour of di-*tert*-butyl-substituted disilanes, we have now undertaken a further structural study on a disilane with three *tert*-butyl groups, 1,1,2-tri-*tert*-butyldisilane, employing the techniques of vibrational spectroscopy, gas-phase electron diffraction and *ab initio* calculations. This system is more crowded than the di-*tert*-butyl substituted disilanes and the structure would be expected to be dominated by steric interactions between these groups.

## Experimental

### Synthesis

A sample of  $\text{Bu}^t_2\text{HSiSiH}_2\text{Bu}^t$  was prepared according to the literature method.<sup>9</sup>

### *Ab initio* calculations

All calculations at the 3-21G\*/SCF<sup>10–12</sup> and 6-31G\*/SCF<sup>13–15</sup> levels were performed on a Dec Alpha 1000 4/200 workstation using the Gaussian 94 program.<sup>16</sup> Calculations at the MP2 level using the 6-31G\* and D95\*<sup>17</sup> basis sets were performed using resources of the U.K. Computational Chemistry Facility, on a DEC 8400 superscalar cluster equipped with 10 fast processors,

† Supplementary data available: Experimental coordinates and parameters for the GED studies and theoretical geometrical parameters. For direct electronic access see <http://www.rsc.org/suppdata/dt/1999/2303/>, otherwise available from BLDSC (No. SUP 57577, 10 pp) or the RSC Library. See Instructions for Authors, 1999, Issue 1 (<http://www.rsc.org/dalton>).

6 GB of memory and 150 GB disk. An extensive search of the torsional potential of 1,1,2-tri-*tert*-butyldisilane was undertaken at the 3-21G\*/SCF level in order to locate all local minima. Three conformers, *syn*, *gauche* and *antiperiplanar*, were located and further geometry optimisations were undertaken at the 6-31G\*/SCF level and at the MP2 level using the 6-31G\* and D95\* basis sets. The D95\* basis set is a *double zeta* basis set that forms molecular orbitals from a linear combination of functions for each atomic orbital and gives a good orbital representation of the first and second row atoms in molecules. Vibrational frequencies were calculated from analytic second derivatives at the 3-21G\*/SCF and 6-31G\*/SCF levels to determine the nature of stationary points for comparison with experimentally determined frequencies, and the force field provided estimates of amplitudes of vibration ( $u$ ) for use in the GED refinements.

### Infrared and Raman spectra

Infrared spectra in the range 3200–300  $\text{cm}^{-1}$  were measured with a Perkin-Elmer 883 spectrometer using a film of pure liquid between CsBr plates. The Raman spectra were recorded with a Jobin Yvon T64000 triple monochromator employing a charge-coupled device (CCD) camera and the 514.5 nm line of an argon-ion laser as the source of excitation. Variable-temperature Raman spectra were obtained by mounting a capillary containing the sample on a copper block equipped with a heater and a thermocouple. Liquid nitrogen was used for cooling the sample.

### Electron diffraction

Electron scattering intensities were recorded on Kodak Electron Image plates using the Edinburgh gas diffraction apparatus operating at *ca.* 44.5 kV (electron wavelength *ca.* 5.6 pm).<sup>18</sup> Nozzle-to-plate distances for the metal inlet nozzle were *ca.* 94 and 259 mm yielding data in the  $s$  range 20–356  $\text{nm}^{-1}$ ; three plates were exposed at each camera distance. The sample and nozzle temperatures were maintained at *ca.* 411 K during the exposure periods.

The scattering patterns of benzene were also recorded for the purpose of calibration; these were analysed in exactly the same way as those for  $\text{Bu}_2\text{HSiSiH}_2\text{Bu}$  so as to minimise systematic errors in the wavelengths and camera distances. Nozzle-to-plate distances, weighting functions used to set up the off-diagonal weight matrix, correlation parameters, final scale factors and electron wavelengths for the measurements are collected in Table S1 (SUP 57577).

The electron-scattering patterns were converted into digital form using a computer-controlled Joyce Loebel MDM6 microdensitometer with a scanning program described elsewhere.<sup>19</sup> The programs used for data reduction<sup>19</sup> and least-squares refinement<sup>20</sup> have been described previously; the complex scattering factors were those listed by Ross *et al.*<sup>21</sup>

## Results

### Theoretical computations

A series of *ab initio* molecular-orbital calculations was undertaken to investigate the structure of 1,1,2-tri-*tert*-butyldisilane (Fig. 1). An extensive search of the torsional potential led to the location of three minima, conformers *syn*,  $\tau[\text{C}(21)\text{--Si}(2)\text{--Si}(1)\text{--H}(13)] = -4.2$ , *gauche*,  $\tau[\text{C}(21)\text{--Si}(2)\text{--Si}(1)\text{--H}(13)] = 63.4$ , and *antiperiplanar*,  $\tau[\text{C}(21)\text{--Si}(2)\text{--Si}(1)\text{--H}(13)] = 163.8^\circ$ . The twist about the silicon–silicon bond is uniquely described by this torsion angle. Vibrational frequency calculations at the 6-31G\*/SCF level confirm that all three forms represent local minima on the potential energy surface. However, the *syn* structure was found to be 10.8  $\text{kJ mol}^{-1}$  lower in energy than the *gauche* structure and 10.3  $\text{kJ mol}^{-1}$  below the *antiperiplanar* structure. This

**Table 1** Theoretical geometrical parameters (D95\*/MP2 level) for the *syn* conformer of 1,1,2-tri-*tert*-butyldisilane<sup>a</sup>

Si(1)–Si(2)	237.5	C(11)–Si(1)–C(12)	118.6
Si(1)–C(11)	192.3	Si(1)–Si(2)–C(21)	112.6
C(11)–C(111)	153.8	Si(2)–C(21)–C(211)	109.7
C(11)–C(112)	154.2	Si(2)–C(21)–C(212)	109.2
C(11)–C(113)	154.2	Si(2)–C(21)–C(213)	110.6
Si(1)–C(12)	192.4	Si(2)–Si(1)–C(11)	110.4
C(12)–C(121)	154.2	Si(1)–C(11)–C(111)	112.2
C(12)–C(122)	153.9	Si(1)–C(11)–C(112)	111.3
C(12)–C(123)	153.9	Si(1)–C(11)–C(113)	107.6
Si(2)–C(21)	191.5	Si(2)–Si(1)–C(12)	108.8
C(21)–C(211)	153.9	Si(1)–C(12)–C(121)	106.8
C(21)–C(212)	154.0	Si(1)–C(12)–C(122)	111.8
C(21)–C(213)	153.9	Si(1)–C(12)–C(123)	112.5
Si(1)–H(13)	150.5	Si(1)–Si(2)–H(22)	110.4
Si(2)–H(22)	149.8	Si(1)–Si(2)–H(23)	110.9
Si(2)–H(23)	149.9	Si(2)–Si(1)–H(13)	107.2
C–H <sup>b</sup>	110.1	C–C–H <sup>b</sup>	111.1
		C(21)–Si(2)–Si(1)–H(13)	–4.2

<sup>a</sup> All distances in pm, all angles in degrees. See Fig. 1 for atom numbering. <sup>b</sup> Average value.

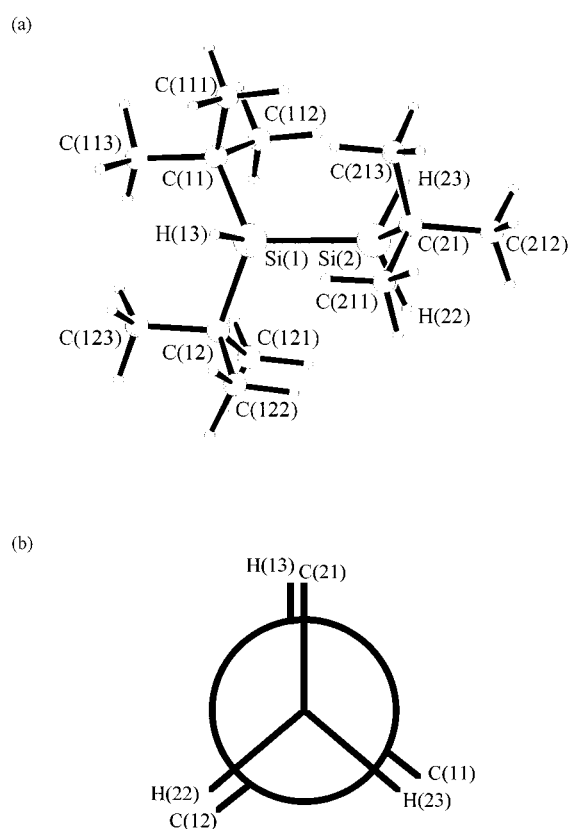


**Fig. 1** (a) Molecular structure and (b) Newman projection of the *syn* conformer, viewed down the Si(2)–Si(1) bond, of  $\text{Bu}_2\text{HSiSiH}_2\text{Bu}$ .

would equate to a mixture containing 96.3% of the *syn* conformer and 2.3% and 1.4% of the *gauche* and *antiperiplanar* conformers, respectively, at room temperature. Attention will therefore be paid mainly to the *syn* structure. The molecular geometry of this conformer for the D95\*/MP2 calculation is presented in Table 1; those calculated at the 3-21G\*/SCF, 6-31G\*/SCF and 6-31G\*/MP2 levels of theory are presented in Table S2 (SUP 57577). The molecular geometries of the *gauche* and *antiperiplanar* conformers calculated at the 3-21G\*/SCF, 6-31G\*/SCF, 6-31G\*/MP2 and D95\*/MP2 levels are presented in Table S3 (SUP 57577), and relative energies are given in Table 2. The nomenclature used to define the three conformers describes the positions of the *tert*-butyl groups at the  $\text{Bu}_2\text{HSi}$  end of the molecule relative to the third *tert*-butyl group.

**Table 2** Relative energies (kJ mol<sup>-1</sup>) of the *syn*, *gauche* and *antiperiplanar* conformers of 1,1,2-tri-*tert*-butyldisilane

Basis Set/Level	<i>syn</i>	<i>gauche</i>	<i>antiperiplanar</i>
3-21G*/SCF	0	12.7	14.8
6-31G*/SCF	0	11.1	12.1
6-31G*/MP2	0	10.1	10.2
D95*/MP2	0	10.8	10.3

As expected, since this system contains no multiple bonds or lone pairs of electrons, the molecular geometry of the conformer proved to be insensitive to changes in the theoretical method. For this reason, only the highest level results (D95\*/MP2) will be discussed.

The molecular geometry of the conformer appears to be dictated predominately by steric interactions, as evident in the calculated values for the C(11)–Si(1)–C(12) angle. In the *syn* conformer, the C(11)–Si(1)–C(12) angle is predicted to be 118.6° compared to 109.5° for an ideal tetrahedral geometry. Further evidence of steric repulsion is found in the value of the Si(1)–Si(2)–C(21) angle, 112.6°. On the other hand, the calculated Si(2)–Si(1)–C(11) angle shows very little deviation from the parent tetrahedral angle of 109.5° (110.4°), as does the Si(2)–Si(1)–C(12) angle (108.8°). The Si(1)–Si(2)–C(21) angle is similar to the Si–Si–C angles calculated for 1,2-di-*tert*-butyldisilane<sup>6</sup> (114.4°). These structural changes relative to the idealised tetrahedral angle of 109.5° serve to reduce the steric interactions in these systems; however, resultant nearest neighbour H···H distances were still predicted to be 219 pm, as compared to 240 pm for the sum of the van der Waals radii of two hydrogen atoms. Internal C–C–C angles indicate that the *tert*-butyl groups are not significantly distorted from local C<sub>3</sub> symmetry. Bond lengths are generally within the expected range based on the results obtained previously for disilanes with *tert*-butyl groups. For example, the Si–Si bond length was predicted to be 237.5 as compared to 236.8 pm in 1,2-di-*tert*-butyldisilane.<sup>6</sup> All the C–C bond lengths fell within the range 153.8–154.2, and the Si–C distances are all in the range 191.5–192.4 pm. These Si–C bond lengths are longer than those of normal Si–C bonds, for example 188.2(1) and 188.6(1) pm for 1,4-disilabutane and 1,5-disilapentane,<sup>22</sup> but compare well with the calculated Si–C bond length in 1,2-di-*tert*-butyldisilane<sup>6</sup> (191.9 pm), which may be a further demonstration of steric interactions in these crowded disilanes, although it could be an electronic effect of the electron-releasing *tert*-butyl groups.

The molecular geometries of the *gauche* and *antiperiplanar* conformers also appear to be dictated predominately by steric interactions, as evident in the predicted values for the Si(1)–Si(2)–C(21) angles. In the *gauche* conformer, the Si(1)–Si(2)–C(21) angle is predicted to be 122.0° and, as might be expected, the same angle is predicted to be even wider in the *antiperiplanar* structure (124.7°) since all the *tert*-butyl groups are in closer proximity in this conformer. Further evidence of steric repulsion is found in the values of the C(11)–Si(1)–C(12) angles in the two conformers, predicted to be 115.8° in the *gauche* conformer but again, as expected, rather wider at 117.5° in the *antiperiplanar* conformer. The Si(2)–Si(1)–C(11) angles in both conformers show a much less dramatic deviation from the parent tetrahedral angle of 109.5° (*gauche* 107.2, *antiperiplanar* 111.5°). The predicted Si(2)–Si(1)–C(12) angles show a larger deviation (*gauche* 113.4, *antiperiplanar* 113.7°) and, again, these angles are similar to Si–Si–C angles calculated for 1,2-di-*tert*-butyldisilane<sup>6</sup> (114.4°). The Si–Si bond lengths were predicted to be 237.3 and 237.6 pm in the *gauche* and the *antiperiplanar* conformers respectively. These bond lengths are very similar to the predicted value for the *syn* conformer and agree well with those found for 1,2-di-*tert*-butyldisilane.<sup>6</sup>

## (b) Vibrational spectra and rotational isomerism

As mentioned above, calculations predict the existence of three conformers, *syn*, *gauche* and *antiperiplanar*, on the potential energy surface of Bu<sup>t</sup><sub>2</sub>HSiSiH<sub>2</sub>Bu<sup>t</sup> with the high energy conformations (*antiperiplanar* and *gauche*) lying 10.3 and 10.8 kJ mol<sup>-1</sup> respectively above the *syn* structure. The GED data can be fitted with the single *syn* structure corresponding to the global minimum. Vibrational spectroscopy should be a slightly more sensitive tool for the detection of the less stable rotamers whose presence in the conformational mixture should be very small according to their predicted energies. In particular, variable-temperature Raman spectroscopy has proven to be an extremely useful tool for conformational analyses as Raman-active skeletal modes are usually very sensitive to the backbone conformation. For example, the energy difference between the *anti* and *gauche* rotamers of MeCl<sub>2</sub>SiSiCl<sub>2</sub>Me has been determined recently from temperature-dependent Raman intensities.<sup>23</sup> In the present study we have recorded the infrared spectrum of liquid Bu<sup>t</sup><sub>2</sub>HSiSiH<sub>2</sub>Bu<sup>t</sup>, variable-temperature Raman spectra in the temperature range from 25 °C to 150 °C, and the Raman spectrum of the solid. Selected vibrational spectra of liquid and solid Bu<sup>t</sup><sub>2</sub>HSiSiH<sub>2</sub>Bu<sup>t</sup> are summarised in Table 3. Calculated and observed vibrational wavenumbers are compared in Table 4.

Using the program ASYM40,<sup>24</sup> the calculated Cartesian Hessian matrices were converted into symmetry force fields resulting in a description of normal modes in terms of symmetry coordinates according to the potential energy distributions. Most of the normal coordinates of the molecule Bu<sup>t</sup><sub>2</sub>HSiSiH<sub>2</sub>Bu<sup>t</sup> are dominated by more than just a single symmetry coordinate and the description given in Table 4 is highly approximate. Its primary use is to help with labelling rather than to permit an accurate visualisation of the vibrational motions.

For reasons of clarity and simplicity high-frequency vibrations involving the methyl groups ( $\nu_{s,as}CH_3$  and  $\delta_{s,as}CH_3$ ) are omitted from Table 4. These vibrations are well known, not sensitive to the conformation around the Si–Si bond and therefore unimportant from the viewpoint of rotational isomerism. The following discussion and characterisation of vibrational frequencies refers explicitly to the global minimum, the *syn* conformer, if not stated otherwise. The eighteen rocking vibrations of the methyl groups occur in three main spectral regions and have been summarised by their respective wavenumber ranges using the labels  $\rho_1CH_3$ ,  $\rho_2CH_3$  and  $\rho_3CH_3$ , respectively. Wavenumber ranges have also been used for the modes  $\nu_{s,as}CC_3$ ,  $\delta_{s,as}CC_3$ ,  $\rho CC_3$  and the torsional vibrations about the C–C single bonds ( $\tau CC$ ), because of the large number of each type of these vibrational modes. Further, calculations predict that the symmetry coordinates  $\rho CC_3$  and  $\tau CC$  are strongly mixed with each other, implying that the torsional vibrations around the C–C bonds, which usually elude observation in the case of smaller molecules like Bu<sup>t</sup>SiX<sub>3</sub> (X = halogen),<sup>25</sup> gain intensity. Therefore, no attempt was made to describe normal modes dominated by both  $\rho CC_3$  and  $\tau CC$  by a single symmetry coordinate and only one wavenumber range for these vibrations has been given.

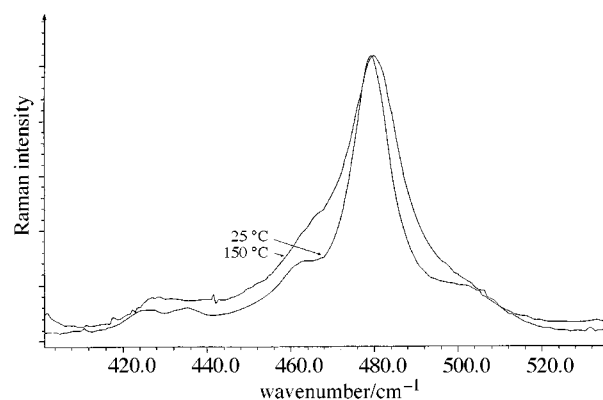
The three rocking vibrations labelled by  $\rho_3CH_3$  correspond to a<sub>2</sub> modes if the *tert*-butyl fragment assumes ideal C<sub>3v</sub> symmetry and therefore are not intense enough to be observed in the IR and Raman. The assignment of the modes  $\nu_s CC_3$  and  $\nu_{as} CC_3$  to experimental wavenumbers is straightforward and agrees well with that made for molecules Bu<sup>t</sup>SiX<sub>3</sub>.<sup>25</sup> The mode  $\delta SiH_2$  appears in the same spectral region as the asymmetric C–C stretching modes  $\nu_{as} CC_3$  and could not be distinguished experimentally from the latter. The wagging mode  $\gamma SiH_2$  is usually of high intensity in the IR but low intensity in the Raman and is assigned to the shoulder at 840 cm<sup>-1</sup> (IR) and the weak Raman band at 841 cm<sup>-1</sup> in the spectrum of the solid. The mode  $\rho SiC_2$  is ascribed to the strong IR band at 793 cm<sup>-1</sup> (792

**Table 3** Vibrational spectra of 1,1,2-*tert*-butyldisilane (<2250  $\text{cm}^{-1}$ )<sup>a</sup>

IR (l, 25 °C)	Raman (l, 25 °C)	Raman (s)
2104vs	2104vvs	2108vvs
2080vs	2080s	2076s
1210 (sh)	—	—
1200s	1201s	1203vs
1188s	1189 (sh)	1192s
1163ms	—	1178 (sh)
1089s	1090vw	1089vw
1070 (sh)	—	—
1035ms	1034vw	1035vw
1012vs	1014w	1015m
—	1003vw	1004vw
935 (sh)	939ms	940s
927vs	928 (sh)	927m
890vw (sh)	888vww	890vww
—	862vww	860vww
840 (sh)	—	841vw
818vs	824s	825vs
—	—	816 (sh)
793vs	794w	792w
770 (sh)	—	—
740 (sh)	730 (sh)	—
707vs, br	710m	711mw
—	—	702mw
656s	654vw	654vw
613m	—	617w
595 (sh)	593vs	594s
575s	575ms	575m
501s	502 (sh)	502w
479m	479s	481s
465vw (sh)	460 (sh)	461w
435ms	434w	434w
—	424w	423vw
410vw	408vww	407vw
387m	—	385 (sh)
—	382m	382m
370m	372 (sh)	370w
—	—	353 (sh)
349s	348w	348w
—	305w	314w
—	272w	281mw, br
—	242w	245w
—	219s	220ms
—	—	206s
—	185vw	187vww
—	—	165 (sh)
—	152w	154w
—	134ms	135m
—	100w	103w

<sup>a</sup> Si–H stretching vibrations are included. Key: vww = very very weak, vw = very weak, w = weak, mw = medium weak, m = medium, ms = medium strong, s = strong, vs = very strong, vvs = very very strong, sh = shoulder, br = broad.

$\text{cm}^{-1}$  in the Raman) and appears at a somewhat lower wavenumber than predicted by the calculations with respect to the position of the  $\nu_s\text{CC}_3$  vibration. The three Si–C stretching modes,  $\nu_{\text{as}}\text{SiC}_2$ ,  $\nu\text{SiC}$  and  $\nu_s\text{SiC}_2$  are readily attributed to the vibrational bands at 613, 595 and 575  $\text{cm}^{-1}$  (IR) or 617, 594 and 575  $\text{cm}^{-1}$  (Raman, solid), respectively. The origin of the strong IR band at 656  $\text{cm}^{-1}$  remains unexplained. As can be seen from Table 4, the modes described by  $\delta\text{SiSiH}$  (angle bending),  $\tau\text{SiH}_2$  (twist),  $\rho\text{SiH}_2$  (rocking) and  $\nu\text{SiSi}$  are predicted to be highly sensitive to the conformation about the Si–Si bond. The modes  $\delta\text{SiSiH}$  and  $\tau\text{SiH}_2$  of the *syn* structure are assigned to the strong and very broad IR peak at 707  $\text{cm}^{-1}$  and the Raman band at 710  $\text{cm}^{-1}$  which splits into two upon solidification (702 and 711  $\text{cm}^{-1}$ ). The shoulder at 740  $\text{cm}^{-1}$  (IR) and the weak shoulder around 730  $\text{cm}^{-1}$  in the Raman spectrum (intensity of the shoulder increasing with temperature) might be due to the mode  $\delta\text{SiSiH}$  of a high energy conformer, perhaps the *antiperiplanar* structure. Similarly, the shoulder at 770  $\text{cm}^{-1}$  (IR) could

**Fig. 2** Portion of the Raman spectrum of liquid  $\text{Bu}^t_2\text{HSiSiH}_2\text{Bu}^t$  at 25 and 150 °C.

also stem from another rotamer (possibly from the *gauche* structure). However, due to the high probability of the presence of strong combination bands or overtones in the IR spectrum of a molecule with 126 fundamental modes care must be taken when stating evidence for the presence of more than just a single rotamer.

A slightly stronger argument in favour of the presence of high energy rotamers in liquid  $\text{Bu}^t_2\text{HSiSiH}_2\text{Bu}^t$  is provided by the appearance of several Raman peaks around 479  $\text{cm}^{-1}$ . The Raman peaks at 479 and 502  $\text{cm}^{-1}$  are assigned to  $\nu\text{SiSi}$  and  $\rho\text{SiH}_2$  of the *syn* conformation, respectively. However, the intensity of the weak shoulder at 460  $\text{cm}^{-1}$  seems to increase slightly with temperature, as shown in Fig. 2, and could be due to one or both of the modes  $\nu\text{SiSi}$  of the high-energy conformations, which are predicted to differ by approximately 20  $\text{cm}^{-1}$  from the value of the *syn* structure. Vibrations below 460  $\text{cm}^{-1}$  do not provide any additional information about rotational isomerism and will not be discussed due to the large number of vibrations and the highly approximate description of these modes by local symmetry coordinates. The lowest wavenumbers corresponding to torsional vibrations around Si–C ( $\tau\text{SiC}$ ) and Si–Si ( $\tau\text{SiSi}$ ) bonds elude observation in the vibrational spectra.

It can be summarised that the present study of the rotational isomerism of  $\text{Bu}^t_2\text{HSiSiH}_2\text{Bu}^t$  employing IR spectroscopy at ambient temperature and variable temperature Raman spectroscopy is consistent with a single conformer, in accordance with the calculations which predict only 2.3% of the *gauche* and 1.4% of the *antiperiplanar* conformers at room temperature. A more sensitive technique like matrix-isolation spectroscopy seems more suitable for unambiguously proving the existence of the three backbone conformers.

### Electron diffraction analysis

On the basis of the *ab initio* calculations described above, electron-diffraction refinements were carried out using a model of the *syn* conformation ( $C_1$  symmetry) to describe the vapour. The conformer is in  $C_1$  symmetry rather than  $C_s$  due to the twists of the *tert*-butyl groups in the  $\text{Bu}^t_2\text{Si}$  fragment to avoid methyl...methyl interactions. The large number of geometric parameters needed to define the model made it necessary to make a number of assumptions including local  $C_{3v}$  symmetry for all methyl groups and local  $C_3$  symmetry for the *tert*-butyl groups. Initially, some of the differences between similar bond lengths and bond angles were restrained using the SARA-CEN<sup>26</sup> method. However, since many of these difference parameters proved to be uncorrelated with other refining parameters, and returned values and e.s.d.s which were close to the restraints, they were fixed in the final refinement. We can therefore be confident that the refined parameters, and their e.s.d.s, are not affected by the assumptions applied to the molecular model.

**Table 4** Calculated and observed wavenumbers for 1,1,2-*tert*-butyldisilane

Approximate description	<i>ab initio</i> (unscaled)			<i>ab initio</i> (scaled by 0.92)			observed (IR, 1, 25 °C) <i>syn</i>	observed (Raman, 1, 25 °C) <i>syn</i>
	<i>syn</i>	<i>gauche</i>	<i>antiperiplanar</i>	<i>syn</i>	<i>gauche</i>	<i>antiperiplanar</i>		
$\nu_s\text{SiH}_2$	2329.1	2335.7	2326.4	2143	2149	2140	2104	2104
$\nu_{as}\text{SiH}_2$	2320.1	2312.6	2319.3	2134	2128	2134	2104	2104
$\nu\text{SiH}$	2298.7	2300.8	2292.5	2115	2117	2109	2080	2080
$\rho_1\text{CH}_3$	1348.9–1316.1	1347.9–1316.7	1348.4–1316.6	1241–1211	1240–1211	1241–1221	1210/1200/1188	1201/1189
$\rho_2\text{CH}_3$	1136.7–1122.7	1136.8–1124.3	1136.4–1123.9	1046–1033	1046–1034	1045–1034	1012	1014/1003
$\rho_3\text{CH}_3$	1052.5–1050.2	1051.6–1048.6	1051.8–1049.0	968–966	967–965	968–965	—	—
$\nu_{as}\text{CC}_3$	1028.3–1017.7	1030.0–1017.8	1030.0–1015.9	946–936	948–936	948–935	935/927	939/928
$\delta\text{SiH}_2$	1042.9	1027.8	1029.0	959	946	947	935 or 927	939 or 928
$\gamma\text{SiH}_2$	923.3	926.3	903.0	849	852	831	840	—
$\nu_s\text{CC}_3$	889.0–883.5	889.8–883.5	889.1–883.9	818–813	819–813	818–813	818	824
$\rho\text{SiC}_2$	878.8	874.0	880.9	808	804	810	793	794
$\delta\text{SiSiH}$	801.4	850.6	825.7	737	783	760	707	710
$\tau\text{SiH}_2$	782.3	772.9	799.2	720	711	735	707	710
$\nu_{as}\text{SiC}_2$	649.1	644.7	649.4	597	593	597	613	593
$\nu\text{SiC}$	628.7	631.1	634.2	578	581	583	595	593
$\nu_s\text{SiC}_2$	611.5	610.2	611.9	563	561	563	575	575
$\rho\text{SiH}_2$	559.3	551.5	540.7	515	507	497	501	502
$\nu\text{SiSi}$	518.3	499.3	500.4	477	459	460	479	479
$\delta_{s,as}\text{CC}_3$	472.7–372.4	459.2–368.6	459.7–360.2	435–343	422–339	423–331	435/387/ 370/349	434/382/ 372/348
$\rho\text{CC}_3, \tau\text{CC}$	342.0–219.7	349.5–218.1	343.8–223.1	315–202	322–201	316–205	—	305/272/ 242/219/ 185
$\delta\text{SiC}_2$	159.9	153.1	145.7	147	141	134	—	152
$\gamma\text{SiC}_2$	136.6	139.3	146.9	126	128	135	—	134
$\tau\text{SiC}_2$	140.4	128.7	129.5	129	118	119	—	134
$\delta\text{SiSiC}$	96.2	87.6	101.1	89	81	93	—	100
$\tau\text{SiC}$	62.6–29.5	100.5–44.0	76.5–48.8	58–27	92–40	70–45	—	—
$\tau\text{SiSi}$	48.2	32.5	26.9	44	30	25	—	—

**Table 5** Refined and calculated geometric parameters for 1,1,2-tri-*tert*-butyldisilane (distances in pm, angles in °) from the GED study<sup>a</sup>

No.	Parameter <sup>b</sup>	GED ( $r_a$ )	D95*/MP2 ( $r_c$ )
$p_1$	C–H	112.4(1)	110.1
$p_2$	C–C	154.5(1)	154
$p_3$	Si–Si	236.3(8)	237.5
$p_4$	Si–C (mean)	191.0(3)	192.1
$p_5$	Si–H (mean)	149.7(10)	150.1
$p_6$	CCH	110.1(6)	111.1
$p_7$	CCC	108.5(2)	108.7
$p_8$	SiSiH average	109.3(11)	109.5
$p_9$	SiSiC average	112.0(6)	110.6
$p_{10}$	SiSiC difference 1	4.8(10)	2.2
$p_{11}$	SiSiC difference 2	7.3(11)	3.8
$p_{12}$	Me twist	58.4(22)	61.4
$p_{13}$	Me tilt	–4.4(11)	—
$p_{14}$	Me rock	2.0(21)	—
$p_{15}$	Bu <sup>t</sup> twist average	62.0(14)	61.5
$p_{16}$	Bu <sup>t</sup> twist difference 1	–12.3(20)	–8.7
$p_{17}$	Bu <sup>t</sup> twist difference 2	–0.3(16)	–1.3
$p_{18}$	Bu <sup>t</sup> rock (gpA)	2.4(11)	—
$p_{19}$	Bu <sup>t</sup> rock (gpB)	4.0(10)	—
$p_{20}$	Bu <sup>t</sup> rock (gpC)	–4.7(9)	—
$p_{21}$	Bu <sup>t</sup> tilt (gpA)	–3.0(10)	—
$p_{22}$	Bu <sup>t</sup> tilt (gpB)	–2.0(9)	—
$p_{23}$	Bu <sup>t</sup> tilt (gpC)	–2.4(10)	—
$p_{24}$	C twist average	112.1(7)	114.1
$p_{25}$	C twist difference 1	–0.3(11)	0.2
$p_{26}$	H twist average	122.0(11)	121.3
$p_{27}$	HSiSiC	–6.2(11)	–4.2

<sup>a</sup> Figures in parentheses are the estimated standard deviations of the last digits. See text for parameter definitions. <sup>b</sup> gpA = *tert*-butyl group with C(21) at centre; gpB = *tert*-butyl group with C(11) at centre; gpC = *tert*-butyl group with C(12) at centre.

The structure of Bu<sup>t</sup><sub>2</sub>HSiSiH<sub>2</sub>Bu<sup>t</sup> was finally defined in terms of twenty-seven independent geometric parameters, comprising five bond lengths, six bond angles and sixteen torsion, rock and tilt parameters (Table 5; atom numbering shown in Fig. 1).

The independent parameters include the C–H and C–C bond lengths ( $p_1$  and  $p_2$ ). Average bond lengths were used for the Si–Si, Si–C and Si–H bond lengths ( $p_3$ – $p_5$ ), with small differences between non-equivalent bond lengths fixed at the *ab initio* values. All C–C–H bond angles ( $p_6$ ) were assumed to be identical, as were all C–C–C bond angles ( $p_7$ ). An average value was adopted for the three Si–Si–H angles ( $p_8$ ), with the small differences from the mean being set at the *ab initio* values. The Si–Si–C angles were defined in terms of an average ( $p_9$ ) of Si(1)–Si(2)–C(21), Si(2)–Si(1)–C(11) and Si(2)–Si(1)–C(12), and two difference parameters, which were included in the refinement procedure since the predicted Si–Si–C angles spanned a wide range of values. The differences were described as the differences between Si(1)–Si(2)–C(21) and Si(2)–Si(1)–C(11) ( $p_{10}$ ) and between Si(1)–Si(2)–C(21) and Si(2)–Si(1)–C(12) ( $p_{11}$ ).

Of the remaining sixteen parameters, nine represent the tilts, rocks and torsions of the three *tert*-butyl groups. These groups were generated by initially placing a methyl group carbon at the origin, with its three H atoms arranged with local  $C_{3v}$  symmetry about the  $x$ -axis and one H in the  $xy$  plane in the positive  $x$  and  $y$  directions. The methyl torsion, tilt and rock parameters, ( $p_{12}$ – $p_{14}$ ) are rotations about the local  $x$ -,  $z$ -, and  $y$ -axes respectively. The methyl group is then translated along the positive  $x$ -axis by the C–C bond length and the central carbon of the *tert*-butyl group is placed at the origin. The correct C–C–C bond angles are generated by rotating the methyl group about the  $z$ -axis, moving the methyl carbon atom in the positive  $y$  direction, and then generating the other methyl groups by rotation of the first group about the  $x$ -axis by 120 or –120°, respectively. The *tert*-butyl torsion angle is a rotation of the group about the  $x$ -axis. Parameters introduced here for the *tert*-butyl torsions include an average ( $p_{15}$ ) of torsions C(211)–C(21)–Si(2)–Si(1), C(111)–C(11)–Si(1)–Si(2), and C(121)–C(12)–Si(1)–Si(2), and two differences. These were the difference between torsion C(211)–C(21)–Si(2)–Si(1) and torsion C(111)–C(11)–Si(1)–Si(2) or C(121)–C(12)–Si(1)–Si(2) ( $p_{16}$  and  $p_{17}$ ).

The rock and tilt parameters are rotations of the whole *tert*-

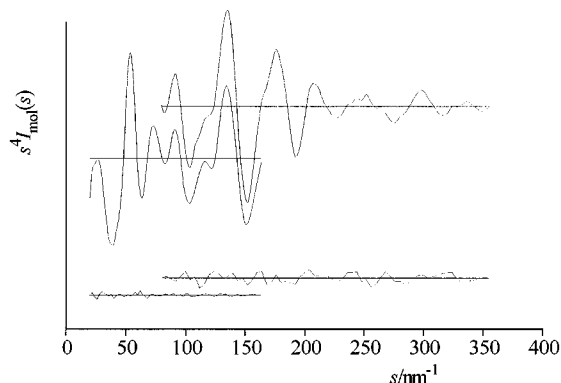


**Fig. 3** Experimental and final weighted difference (experimental – theoretical) molecular-scattering intensities for 1,1,2-tri-*tert*-butyl-disilane.

butyl groups about the *y*-axis and the *z*-axis respectively. Three individual rocks ( $p_{18}$ – $p_{20}$ ) and three individual tilts ( $p_{21}$ – $p_{23}$ ) were introduced here for the *tert*-butyl groups with C(21), C(11) and C(12) as the central atoms of the groups. A positive rock would move the *tert*-butyl group with C(21) at the centre away from that with C(12) at the centre whilst the *tert*-butyl with C(11) at the centre would be moved towards C(12) and C(12) would be moved away from C(11), all in the local *y* direction of the *tert*-butyl groups. Positive tilts would move the *tert*-butyl groups at one end of the molecule towards the group at the other end in the local *z* direction, and *vice versa*.

Having generated the *tert*-butyl groups in their local coordinate systems, they need to be rotated about the *x*-axis to put them in the correct position relative to the silicon atoms. The two *tert*-butyl groups and the hydrogen attached to Si(1) were initially placed in the *xy* plane, and the *tert*-butyl groups were then rotated about the *x*-axis. These rotations are defined in terms of an average of C(11)–Si(1)–Si(2)–H(13) and C(12)–Si(1)–Si(2)–H(13) ( $p_{24}$ ) and a difference between torsion C(11)–Si(1)–Si(2)–H(13) and torsion C(12)–Si(1)–Si(2)–H(13) ( $p_{25}$ ).

The *tert*-butyl group and H atoms attached directly to Si(2) were placed in the *xy* plane and the two hydrogen atoms were then rotated about the *x*-axis in opposite directions by torsions H(22)–Si(2)–Si(1)–C(21) and H(23)–Si(2)–Si(1)–C(21). The average of these two dihedrals is ( $p_{26}$ ) and the difference was set at the *ab initio* value.

Finally, the dihedral angle C(21)–Si(2)–Si(1)–H(13) ( $p_{27}$ ) described the overall conformation about the Si–Si bond, with a value of zero indicating the conformation in which the hydrogen of the Bu<sup>t</sup><sub>2</sub>HSi group and the carbon of the Bu<sup>t</sup><sub>2</sub>HSi group were eclipsing one another.

The starting parameters for the  $r_a$  refinement were taken from the theoretical geometry optimised at the D95\*/MP2 level. The  $R_G$  structure was not refined due to the fact that the rectilinear vibrational corrections (*i.e.* parallel and perpendicular correction terms) are known to be unreliable for a molecule this size with many low lying vibrational modes. Theoretical (6-31G\*/SCF) Cartesian force fields were obtained and converted into force fields described by a set of symmetry coordinates using a version of the ASYM40 program<sup>24</sup> modified to work for molecules with more than forty atoms. All geometric parameters were then refined.

In total twenty-seven geometric parameters and forty-three groups of vibrational amplitudes were refined. Flexible restraints were employed during the refinement using the SARACEN method.<sup>26</sup> In total, twenty-one geometric and thirty-seven amplitude restraints were employed. These are listed in Tables S4 and S5 (SUP 57577).

The success of the final refinement, for which  $R_G = 0.060$  ( $R_D = 0.052$ ), can be assessed on the basis of the molecular scattering intensity curves (Fig. 3) and the radial distribution curve (Fig. 4). Final refined parameters are listed in Table 5,

**Table 6** Selected interatomic distances and mean amplitudes of vibration for 1,1,2-tri-*tert*-butyl-disilane from the GED study<sup>a</sup>

No.	Atom pair	$r_a/\text{pm}$	$u/\text{pm}$
1	Si(1)–Si(2)	236.3(8)	7.2(6)
2	Si(2)–C(21)	190.4(3)	6.1(7)
3	Si(1)–C(11)	191.7(3)	6.2(6)
4	Si(1)–C(12)	191.3(3)	6.2(6)
5	Si(2)–H(23)	149.3(10)	9.4(2)
6	Si(2)–H(22)	149.7(10)	9.4(tied to $u_5$ )
7	Si(1)–H(13)	150.0(10)	9.4(tied to $u_5$ )
8	C–C	154.5(1)	5.2(2)
9	C–H	112.4(1)	6.9(2)
10	C(21)⋯H(2111)	220.7(25)	9.7(12)
11	C(211)⋯C(212)	250.8(3)	7.3(5)
12	Si(1)⋯C(21)	362.7(14)	13.9(12)
13	Si(2)⋯C(211)	283.3(19)	10.7(5)
14	Si(2)⋯C(212)	278.6(17)	10.3(7)
15	Si(2)⋯C(213)	289.8(18)	10.9(7)
16	Si(2)⋯C(11)	354.1(19)	14.0(12)
17	Si(1)⋯C(111)	279.7(18)	10.3(7)
18	Si(1)⋯C(112)	292.4(16)	10.7(7)
19	Si(1)⋯C(113)	282.8(16)	10.8(7)
20	Si(2)⋯C(12)	348.5(18)	12.8(9)
21	Si(1)⋯C(121)	293.5(51)	10.4(7)
22	Si(1)⋯C(122)	279.4(53)	10.2(7)
23	Si(1)⋯C(123)	280.8(106)	10.0(7)
24	C(11)⋯C(12)	333.4(20)	10.0(11)

<sup>a</sup> See Fig. 1 for atom numbering. (Other atom pairs were also used in the refinement but are not shown here.)

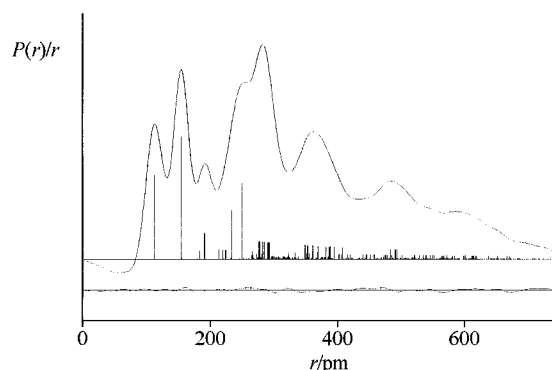


**Fig. 4** Experimental and difference (experimental – theoretical) radial-distribution curves,  $P(r)/r$ , for Bu<sup>t</sup><sub>2</sub>HSiSiH<sub>2</sub>Bu<sup>t</sup>. Before Fourier inversion the data were multiplied by  $s \cdot \exp(-0.00005s^2)/(Z_{\text{Si}} - f_{\text{Si}})/(Z_{\text{C}} - f_{\text{C}})$ .

interatomic distances and the corresponding amplitudes of vibration in Table 6, with the least-squares correlation matrix shown in Table S6 and the experimental coordinates from the GED analysis in Table S7 (SUP 57577). In the SARACEN analysis, all correlation between refining parameters is included in the error estimates by the use of flexible restraints. We therefore quote the estimated standard deviations,  $\sigma$ , and believe that these are realistic estimates of the uncertainties of the parameters.

Fig. 1 shows a perspective view of the *syn* conformer of Bu<sup>t</sup><sub>2</sub>HSiSiH<sub>2</sub>Bu<sup>t</sup> in the optimum refinement of the GED data with a Newman projection along the Si–Si bond vector showing the *syn* conformation.

## Discussion

Theoretical and experimental studies show that 1,1,2-tri-*tert*-butyl-disilane exists essentially as a single *syn* conformer in the gas phase. The electron diffraction data for the compound were fitted using the SARACEN<sup>26</sup> method on the basis of such an *syn* structure.

The vibrational spectra do not change significantly with changes in the temperature, indicating the presence of one con-

former. Spectroscopic studies are therefore consistent with the GED experiment and theory, but do not unambiguously prove that there is only one conformer present in the vapour.

The final experimental structure is in good agreement with that calculated *ab initio* at the D95\*/MP2 level; computed bond lengths and angles generally fall within 1–2 pm or 1–2° of the GED values (Table 5). For example, the Si–Si bond length refined to 236.3(8) pm as compared to the computed value of 237.5 pm. The mean C–C bond length refined to 154.5(1) pm compared to 154.0 pm (mean) from the calculations and the experimental range of Si–C bond lengths was 190.4–191.7 pm compared to the calculated range of 191.5–192.4 pm. However, the Si(1)–Si(2)–C(21) bond angle refined to 116.0(8)°, a lot wider than the predicted value of 112.6°, and the C(11)–Si(1)–C(12) bond angle refined to 121.1(11)° compared to the calculated value of 118.6°. Both these observations serve to highlight the significant steric interactions within the molecule. The torsion about the Si–Si axis, dihedral angle C(21)–Si(2)–Si(1)–H(13), which uniquely describes the position of all the groups about the Si–Si axis, agrees reasonably well with the predicted value;  $-6.2(11)^\circ$  vs.  $-4.2^\circ$ .

Observed geometric parameters are generally consistent with those for a number of other closely related compounds. For example, the Si–Si bond distance in the *syn* conformer of 1,1,2-tri-*tert*-butyldisilane [236.3(8) pm] is within the range of values found for other disilanes from GED refinements including 1,2-di-*tert*-butyldisilane<sup>6</sup> [234.8(3) pm], 1,1,2,2-tetrabromodisilane<sup>4</sup> [234.9(19) pm], 1,2-diiododisilane<sup>5</sup> [238.0(34) pm] and 1,1,2,2-tetraiododisilane<sup>5</sup> [238.9(37) pm], but a little longer as might be expected, either on steric or electronic grounds, with the *tert*-butyl groups being electron-donating. Refined values of the C–C [154.5(1) pm] and Si–H [149.7–150.0 pm] bond lengths are in excellent agreement with calculated values and compare well with other previously reported bond lengths,<sup>22</sup> as would be expected.

The most striking feature of the structure is the deviation of the C(11)–Si(1)–C(12) bond angle from the “pure” sp<sup>3</sup> tetrahedral angle [109.5°] by 11.6°. This provides evidence of steric strain and the wide angle observed is probably caused by the close proximity of two of the *tert*-butyl groups at one end of the molecule. It also reflects the easy deformation of angles at silicon, which allows the accommodation of several large substituents. Another structural feature of note is the value obtained for the Si(1)–Si(2)–C(21) bond angle [116.0(8)°]. This angle is similar to those previously observed for 1,2-di-*tert*-butyldisilane<sup>6</sup> [113.7(3)°] and 1,2-di-*tert*-butyltetrafluorodisilane<sup>7</sup> [114.6(7)°] and provides evidence for significant steric interaction in all the *tert*-butyldisilanes due to the individual *tert*-butyl groups.

Much larger Si(1)–Si(2)–C(21) bond angles are observed in the *gauche* and *antiperiplanar* conformers [122.5(8) and 125.2(9)° respectively]. This can be attributed to the closer interactions between the *tert*-butyl groups at either end of the molecule. The values of the C(11)–Si(1)–C(12) angles refined to 114.5(9) for the *gauche* conformer and 117.2(8)° for the *antiperiplanar* conformer. These are smaller than that observed for the *syn* conformer but are still significantly distorted from the idealised tetrahedral angle, again indicating the easy deformation of angles at silicon atoms to accommodate bulky substituents.

In the early stages of this analysis, before the existence of the *syn* conformer had been recognised, the experimental data were also fitted with a mixture of the other two conformers, *gauche* { $\tau$ [C(21)–Si(2)–Si(1)–H(13)] = 63.4} and *antiperiplanar* { $\tau$ [C(21)–Si(2)–Si(1)–H(13)] = 163.8°}, in equal amounts, as predicted *ab initio*. All geometric parameters were then refined before determining the relative weights of the two conformations. The final weight of the *gauche* conformer was thus determined to be 50.8% with a standard deviation of 3.2% according to the Hamilton test for this parameter.<sup>27</sup> From the

final refinement, for which  $R_G = 0.057$  ( $R_D = 0.054$ ), it can be seen that this two conformer model fits the experimental data as well as the single *syn* model. This demonstrates that caution must be exercised when initially exploring the potential energy surface to locate all structurally stable minima and to determine the differences in energy between them. The two-conformer model used forty-two independent geometric parameters comprising five bond lengths, nine bond angles and twenty-eight torsion, rock and tilt parameters. This large number of refinable parameters probably contributed to the overall goodness of fit of these two conformers compared to the single *syn* conformer. Mixtures of all three conformers will also fit the data well. However, we believe that the refinement based on the *syn* conformer alone is the most satisfactory result, in the light of all available information, both theoretical and experimental.

## Acknowledgements

We thank the EPSRC for financial support of the Edinburgh Electron Diffraction Service (grant GR/K44411), for the provision of microdensitometer facilities at the Daresbury Laboratory and for the Edinburgh *ab initio* facilities (grant GR/K04194). We also thank Dr. V. Typke of the University of Ulm for the variable-array version of ASYM40, and the U.K. Computational Chemistry Facility (admin: Department of Chemistry, King's College London, Strand, London WC2R 2LS) for the computing time on Columbus.

## References

- 1 R. D. Miller and J. Michl, *Chem. Rev.*, 1989, **89**, 1359.
- 2 See, for example, B. Albinsson, H. Teramae, J. W. Downing and J. Michl, *Chem. Eur. J.*, 1996, **2**, 529.
- 3 V. S. Mastryukov, in *Stereochemical Applications of Gas-Phase Electron Diffraction*, eds. I. Hargittai and M. Hargittai, VCH, Weinheim, 1990, vol. B, p. 1.
- 4 H. Thomassen, K. Hagen, R. Stølevik and K. Hassler, *J. Mol. Struct.*, 1986, **147**, 331.
- 5 E. Røhmen, K. Hagen, R. Stølevik, K. Hassler and M. Pöschl, *J. Mol. Struct.*, 1991, **244**, 41.
- 6 D. Hnyk, R. S. Fender, H. E. Robertson, D. W. H. Rankin, M. Bühl, K. Hassler and K. Schenzel, *J. Mol. Struct.*, 1995, **346**, 215.
- 7 B. A. Smart, H. E. Robertson, N. W. Mitzel, D. W. H. Rankin, R. Zink and K. Hassler, *J. Chem. Soc., Dalton Trans.*, 1997, 2475.
- 8 S. L. Hinchley, B. A. Smart, C. A. Morrison, H. E. Robertson, D. W. H. Rankin, R. Zink and K. Hassler, unpublished results.
- 9 B. Reiter and K. Hassler, *J. Organomet. Chem.*, 1994, **467**, 21.
- 10 J. S. Binkley, J. A. Pople and W. J. Hehre, *J. Am. Chem. Soc.*, 1980, **102**, 939.
- 11 M. S. Gordon, J. S. Binkley, J. A. Pople, W. J. Pietro and W. J. Hehre, *J. Am. Chem. Soc.*, 1982, **104**, 2797.
- 12 W. J. Pietro, M. M. Francl, W. J. Hehre, D. J. DeFrees, J. A. Pople and J. S. Binkley, *J. Am. Chem. Soc.*, 1982, **104**, 5039.
- 13 W. J. Hehre, R. Ditchfield and J. A. Pople, *J. Chem. Phys.*, 1972, **56**, 2257.
- 14 P. C. Hariharan and J. A. Pople, *Theor. Chim. Acta*, 1973, **28**, 213.
- 15 M. S. Gordon, *Chem. Phys. Lett.*, 1980, **76**, 163.
- 16 M. J. Frisch, G. W. Trucks, H. B. Schlegel, P. M. W. Gill, B. G. Johnson, M. A. Robb, J. R. Cheesman, T. A. Keith, G. A. Petersson, J. A. Montgomery, K. Raghavachari, M. A. Al-Laham, V. G. Zakrzewski, J. V. Ortiz, J. B. Foresman, J. Cioslowski, B. B. Stefanov, A. Nanayakkara, M. Challacombe, C. Y. Peng, P. Y. Ayala, W. Chen, M. W. Wong, J. L. Andres, E. S. Replogle, R. Gomperts, R. L. Martin, D. J. Fox, J. S. Binkley, D. J. Defrees, J. Baker, J. P. Stewart, M. Head-Gordon, C. Gonzalez and J. A. Pople, Gaussian 94 (Revision C.2), Gaussian Inc., Pittsburgh, PA, 1995.
- 17 T. H. Dunning, Jr. and P. J. Hay, in *Modern Theoretical Chemistry*, ed. H. F. Schaefer III, Plenum Press, New York, 1976, p. 1.
- 18 C. M. Huntley, G. S. Laurensen and D. W. H. Rankin, *J. Chem. Soc., Dalton Trans.*, 1980, 954.
- 19 S. Cradock, J. Koprowski and D. W. H. Rankin, *J. Mol. Struct.*, 1981, **77**, 113.
- 20 A. S. F. Boyd, G. S. Laurensen and D. W. H. Rankin, *J. Mol. Struct.*, 1981, **71**, 217.

- 21 A. W. Ross, M. Fink and R. Hilderbrandt, in *International Tables for Crystallography*, ed. A. J. C. Wilson, Vol. C, Kluwer Academic Publishers, Dordrecht, 1992, p. 245.
- 22 See, for example, N. W. Mitzel, B. A. Smart, A. J. Blake, H. E. Robertson and D. W. H. Rankin, *J. Phys. Chem.*, 1996, **100**, 9339.
- 23 For example, see M. Ernst, K. Schenzel, A. Jähn and K. Hassler, *J. Mol. Struct.*, 1997, **412**, 83.
- 24 L. Hedberg and I. M. Mills, *J. Mol. Spectrosc.*, 1993, **160**, 117.
- 25 R. Zink and K. Hassler, *Spectrochimica Acta, Part A*, 1999, **55**, 333.
- 26 A. J. Blake, P. T. Brain, H. McNab, J. Miller, C. A. Morrison, S. Parsons, D. W. H. Rankin, H. E. Robertson and B. A. Smart, *J. Phys. Chem.*, 1996, **100**, 12280; P. T. Brain, C. A. Morrison, S. Parsons and D. W. H. Rankin, *J. Chem. Soc., Dalton Trans.*, 1996, 4589.
- 27 W. C. Hamilton, *Acta Crystallogr.*, 1965, **18**, 502.

*Paper 9/02342I*